August 27-31, 2023
FLORENCE - ITALY
ICWE 16
16th International Conference on Wind Engineering

Reynolds-number effects in flow around a pair of circular cylinders in crossflow up to $\mathrm{Re} \approx 10^7$

Günter Schewe[1], Marc Braune[2], Nils van Hinsberg[3], Holger Mai[4]

[1] *DLR - Institute of Aeroelasticity, Göttingen, Germany, Guenter.Schewe@dlr.de*
[2] *DLR - Institute of Aeroelasticity, Göttingen, Germany, Marc.Braune@dlr.de*
[3] *DLR - Institute of Aerodynamics and Flow Technology, Göttingen, Germany, Nils.vanHinsberg@dlr.de*
[4] *DLR - Institute of Aeroelasticity, Göttingen, Germany, Holger.Mai@dlr.de*

SUMMARY:
Steady and unsteady force measurements were performed on a pair of tandem circular cylinders in cross flow (spacing $S/d = 1.56$, 2.8, and 4) for Reynolds-Nos. from sub- up to transcritical values ($\mathrm{Re} \approx 10^7$). The tests were carried out in the High Pressure Wind Tunnel in Göttingen. In addition to the analysis of the spectra, Strouhal-Nos., etc., for $S/d = 1.56$ the dependence of the angle of incidence α was also investigated. These curves exhibited a high degree of nonlinearity. In the transcritical Reynolds-No. range flow induced vibrations were observed.

Keywords: tandem circular cylinders, high Reynolds numbers, flow induced vibrations

1. INTRODUCTION

Knowlegde of the flow around a pair of circular cylinders is of great importance for technical applications like flows around cables, large wind-engineering- or offshore structures. For these problems, achievement of the prototype Reynolds-No. is of great importance. The presentation summarizes the results of the experiments (Schewe and Jacobs, 2019; Schewe, van Hinsberg, et al., 2021) performed in the High Pressure Wind Tunnel in Göttingen (HDG), where the Reynolds-No. can be varied over three orders of magnitude by merely varying the flow parameters. The experiments have been performed for spacing distances between the cylinder centres $S/d = 1.56$, 2.8, and 4. Apart from the mean forces on both cylinders, the fluctuating forces acting on the downstream cylinder were analyzed. Thus, information on the spectra, Strouhal-Nos., and RMS-values was obtained. In addition, the data were subjected to a wavelet analysis to reveal information about the time-frequency behavior of the phenomena. For $S/d = 1.56$ the dependence of the angle of incidence α was also investigated which exhibited a high degree of nonlinearity. The distance and the Reynolds-No. have strong influence on the flow topology and determine whether the two cylinders behave like one extended bluff body or like two clearly separated ones. If S is small, negative drag forces can occur on the downstream cylinder. When increasing S, a jump to positive drag forces will appear (drag inversion) at the so-called critical spacing S_c. For a small distance ($S/d = 1.56$), it is shown that the critical spacing S_c depends on the Reynolds-No. range and that a drag inversion also occurs at transcritical Re. In addition, a drag inversion is an indication for a change in modes and can thus be a source of instability.

2. DRAG COEFFICIENTS

Fig. 1 shows that in all three cases S/d the drag-curves for the front cylinder $Cd_1(\mathrm{Re})$ are similar to those for a single smooth circular cylinder. The curves $Cd_2(\mathrm{Re})$ of the downstream cylinder exhibit an inverse development. For $S/d = 1.56$ at the critical Reynolds-No., a sudden change in drag occurs. For $S/d = 2.8$, the change is less drastic. In the subcritical regime the negative sign indicates that $S/d = 1.56$ and 2.8 are below the critical spacing Sc. Thus, the state belongs to the reattachment regime (mode I), where one common vortex street is formed. However, for

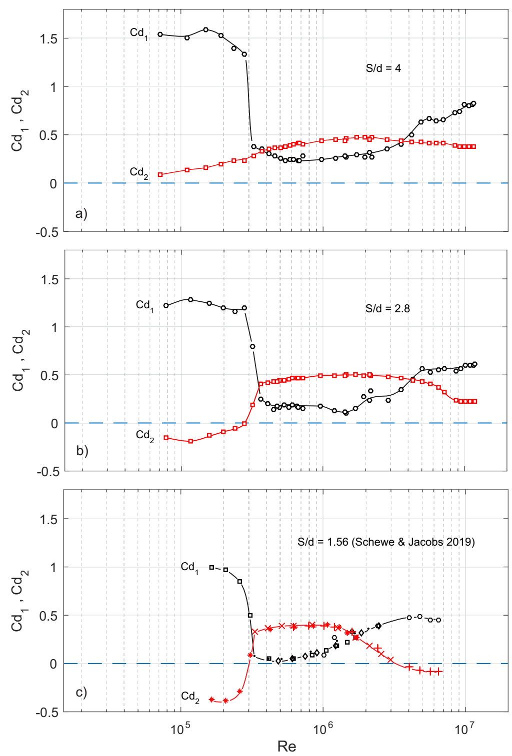

Figure 1. Drag coefficients for both individual cylinders (Schewe, van Hinsberg, et al., 2021).

$S/d = 4$ there is no zero-crossing $\rightarrow$ co-shedding mode (mode II). For supercritical Reynolds-Nos., the drag on the downstream cylinder is higher than on the upstream one in all three cases. In the upper transition (super-/transcritical) the separation bubbles gradually disappear, leading to a renewed increase of Cd_1 and a reduction of Cd_2. For $S/d = 1.56$ at $\mathrm{Re} \approx 10^6$, there is a second zero-crossing of $Cd_2 \rightarrow -0.07$ (co-shedding mode II back to mode I). For $S/d = 2.8$, the trend of the curve is similar, but the decline is not as steep and Cd_2 remains positive. For $S/d = 4$, a distinctive dip of the drag curve $Cd_2(\mathrm{Re})$ does not exist.

3. STROUHAL-NUMBERS AND RMS-VALUES

For $S/d = 2.8$ and 4, the Strouhal-Nos. St and the RMS-values Cl_{rms} are strongly depending on the Reynolds-No., which is depicted in Fig. 2. At the critical Reynolds-No. there is a jump to the supercritical state with a dominant peak at $\mathrm{St} = 0.44$ and a secondary peak at $\mathrm{St} = 0.24$.

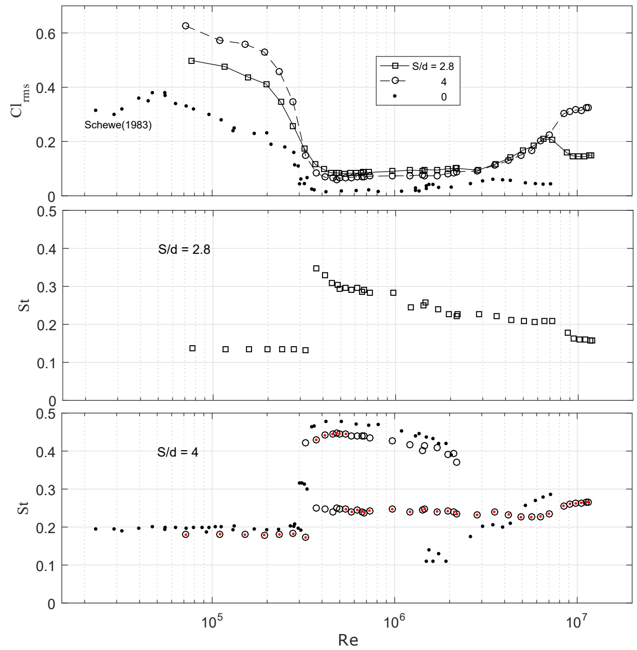

Figure 2. RMS-values and Strouhal-numbers: In the supercritical range two peaks occurred. The dominant peaks are indicated by dots within the circular symbols and open circles without dots belong to secondary peaks (Schewe, van Hinsberg, et al., 2021).

Considering only the high values around St ≈ 0.4, it can be seen that these are quite close to the case of the single smooth cylinder. For $S/d = 2.8$, the curve St(Re) of the downstream cylinder is quite different. The jump in the supercritical range reaches only St ≈ 0.34, followed by a gradual decrease down to St ≈ 0.2. At around Re $\approx 8 \cdot 10^6$ there is a distinctive dip down to a level of St ≈ 0.16.

4. VIBRATIONS IN THE TRANSCRITICAL RANGE

For the smallest distance $S/d = 1.56$ in the transcritical Re range, vibrations occurred around $\alpha = 0°$ for the front cylinder. A conventional strain gauge balance was installed only for this case, which is not ideally rigid. This leads to degrees of freedom for the cylinder. Fig. 3 shows the lift- and drag coefficient as a function of α for Re $\rightarrow 6 \cdot 10^6$. From Re $= 3.4 \cdot 10^6$, there was a range of angles where also violent vibrations occurred. The observed vibrations of the front cylinder around $\alpha = 0°$ are likely caused by vortex resonance and perhaps they are coupled with the mentioned drag-inversion at very high Reynolds-numbers. The reasons for the vibrations of the downstream cylinder for $\alpha \neq 0$ are not clear – perhaps it is wake galloping.

5. FLOW TOPOLOGY

Fig. 4 displays tentative sketches of the flow topology. At subcritical Reynolds-Nos. (first column), for $S/d = 1.56$ and 2.8, the two cylinders can be seen as one extended body (mode I). Suction effects in the gap cause negative drag ($Cd_2 = -0.4$). For $S/d = 2.8$, the separated free shear layers can reattach on the downstream cylinder. In both cases dominate proximity effects $\rightarrow$ one vortex street (mode I). For $S/d = 4$, both cylinders generate vortices (co-shedding regime,

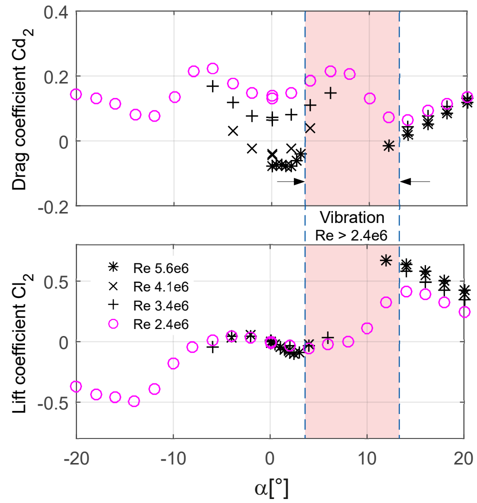

Figure 3. Lift and drag coefficient of the downstream cylinder for transcritical Reynolds-Nos. ($S/d = 1.56$, Messina cable). The arrows indicate how we approached the red vibration range (Schewe and Jacobs, 2019).

mode II). Larger distance $\rightarrow$ the suction effect is diminished and the drag is thus positive $Cd_2 > 0$. At supercritical Reynolds-Nos. (second column), for $S/d = 1.56$ and 2.8, the transition is accompanied by a sign reversal $\rightarrow$ crossover from mode I to co-shedding mode II. Thus now for all three cylinder distances Cd_2 is positive $\rightarrow$ co-shedding mode. At transcritical Reynolds-Nos. (third col-

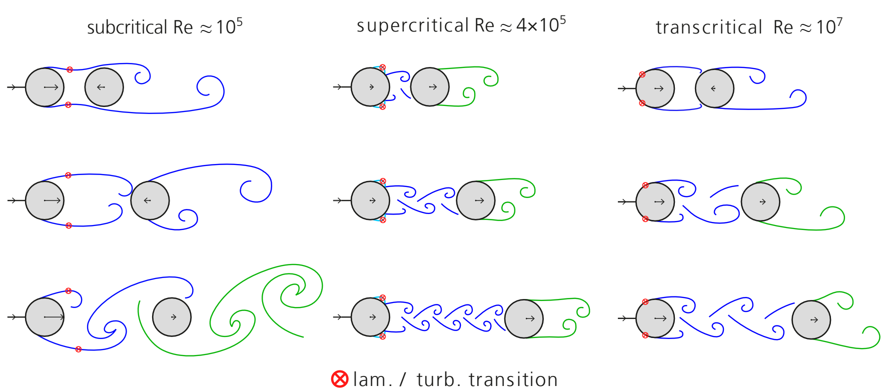

Figure 4. Simplified sketches of the instantaneous 2d flow fields (Schewe, van Hinsberg, et al., 2021). The key role is played by the location of the laminar/turbulent transition, which moves upstream for increasing Re, and the formation of separation bubbles.

umn), now the transition at the upstream cylinder has reached the front side. For $S/d = 1.56$, the flow thus changes once again (back to mode I) followed by a second zero-crossing of Cd_2. For $S/d = 2.8$ and 4, the larger S results in weaker proximity effects, thus both latter cases belong to the co-shedding mode II.

REFERENCES

Schewe, G. and Jacobs, M., 2019. Experiments on the flow around two tandem circular cylinders from sub- up to transcritical Reynolds numbers. Journal of Fluids and Structures 88, 148–166.

Schewe, G., van Hinsberg, N., and Jacobs, M., 2021. Investigation of the steady and unsteady forces acting on a pair of circular cylinders in crossflow up to ultra-high Reynolds numbers. Experiments in Fluids 62.